J. Membrane Biol. 138, 209–219 (1994)

The Journal of
Membrane
Biology

Satellite Glial Cell Responses to Neuronal Firing in the Nervous System of *Helix pomatia*

I. Gommerat, M. Gola

Laboratoire de Neurobiologie, C.N.R.S., 31, Chemin Joseph Aiguier, 13402 Marseille Cedex 20, France

Received: 29 July 1993/Revised: 23 November 1993

Abstract. Patch clamp experiments were conducted on satellite glial cells attached to the cell body of neurons in place within the nervous system of the snail *Helix pomatia*. The glial cells were studied using cell-attached and whole-cell patch clamp configurations while the underlying neurons were under current or voltage clamp control.

The resting potential of the glial cells (−69 mV) was more negative than that of the underlying neurons (−53 mV), due to their high K^+ selectivity. Densely packed K^+ channels were present, some of which were active at the cell resting potential. Neuronal firing elicited a cumulative depolarization of the glial cells. Large K^+ currents flowing from V-clamped neurons depolarized the glial layer by up to 30 mV. The glial depolarization was directly correlated with the size of the neuronal K^+ current. The glial cells recovered their resting potential within 2–5 sec. The neuronal depolarization induced a delayed (20–30 sec) and persistent (3–4 min) increase in the glial K^+ channel opening probability. Likewise, pulses of K^+ (20–50 mM)-rich saline activated the glial channels, unless the underlying neuron was held hyperpolarized. In low Ca^{2+}-high Mg^{2+} saline, neuron depolarization and K^+-rich saline did not activate the glial K^+ channels.

These data indicate that a calcium-dependent signal released from the neuronal cell body was involved in glial channel regulation. Neuron-induced channel opening may help eliminate the K^+ ions flowing from active neurons.

Key words: Glial cells — Potassium channels — *Helix pomatia* — Neuronal-glial interactions

Correspondence to: M. Gola

Introduction

Among the various roles that glial cells may play in the nervous system, it has been established that they take up the excess K^+ resulting from neuronal activity. Several processes help to limit the increase in $[K^+]_o$ produced by active neurons: diffusion through the extracellular space, active pumping and passive uptake by glial cells permeable to K^+. This concept was put forward by Kuffler, Nicholls and Orkand (1966) and Orkand, Nicholls and Kuffler (1966) who discovered that glial cells have a high potassium conductance. These authors suggested the existence of a "spatial buffering" mechanism whereby potassium enters glial cells in regions exposed to high external potassium and flows to remote regions of the glial syncytium which are not exposed to potassium increases. Studies on the K^+ dynamics in specialized glial cells in insect and vertebrate retina have indicated that the "spatial buffering" mechanism plays an important role in controlling $[K^+]_o$ (*review by* Newman, 1986). Bevan et al. (1985) have suggested an alternative mechanism which involves the entry of both potassium and chloride into the glial cells. This would allow potassium ions to accumulate near the site of entry rather than flowing in remote areas (for review, *see* Walz, 1989; Barres, 1991).

The mechanisms of potassium buffering by glial cells, except those involving active uptake, require a high potassium conductance enabling potassium ions to move passively propelled by the local driving force. During the last decade, the K^+ channels present in glial cells have been thoroughly documented (*review by* Barres, Chun & Corey, 1990; Chiu, 1991; Ritchie, 1992). They have been detected in either whole-cell currents or at the single level in astrocytes (Bevan & Raff, 1985; Sonnhof & Schachner, 1986; Nowak, Ascher & Berwald-Netter, 1987; Barres, Chun & Corey, 1988; Jalonen & Holopainen, 1989), oligodendrocytes (Kettenmann et al., 1982; Kettenmann, Orkand & Lux,

1984; Barres et al., 1988; Soliven et al., 1988; Sontheimer & Kettenmann, 1988; McLarnon & Kim, 1989), Schwann cells (Chiu, Shrager & Ritchie, 1984; Konishi, 1989; Wilson & Chiu, 1990; Amédée et al., 1991), retinal Müller cells (Brew et al., 1986; Nilius & Reichenbach, 1988), glial cells within hippocampal slices (Steinhaüser et al., 1992) and satellite glial cells in prevertebral sympathetic ganglia (Gola et al., 1993).

Among the various K^+ channels, those exhibiting inwardly rectifying properties are clearly candidates for dealing with the potassium uptake. Inward-rectifier channels have indeed been detected in retinal Müller cells (Brew et al., 1986), cultured oligodendrocytes (McLarnon & Kim, 1989) and astrocytes (Barres et al., 1988), mammalian Schwann cells (Wilson & Chiu, 1990; Chiu, 1991) and satellite glial cells in the peripheral nervous system (Gola et al., 1993).

Most of the data on individual K^+ channel properties have been collected on cultured or acutely isolated glial cells (however, *see* Berger, Schnitzer & Kettenmann, 1991; Marrero et al., 1991 and Gola et al., 1993). There exist few direct data relative to the way these channels may be regulated by neuronal activity in intact tissues. Glial cells have receptors for many neurotransmitters and neuropeptides, which indicates that they can receive information from neighboring neurons (Murphy & Pearce, 1987). Unidentified signals released by active neurons have been thought to open the chloride channels (Barres et al., 1990) involved in the Bevan model and to alter the Na^+ channels in astrocytes in the frog optic nerve (Marrero et al., 1989).

The aim of the present study was to evaluate whether neuronal activity and the consecutive increase in $[K^+]_o$ alter the properties of the associated glial cells. For this purpose, we developed a preparation in which patch clamp recordings could be performed on satellite glial cells attached to the cell body of a neuron in place within the nervous system of the mollusc *H. pomatia.*

Materials and Methods

The experiments were conducted on satellite glial cells attached to the cell body of neurons within the nervous system of the mollusc *H. pomatia.* Methods for cleaning the ganglia from the connective sheaths while preserving the glial cell layer covering the neurons have been previously described (Gommerat et al., 1993). Most of the experiments were conducted on the large nerve cell bodies located in the caudal part of the visceral ganglion, including the P cells (Pin et al., 1990), which were easily identified from their long-lasting depolarization in response to repeated firing.

Glial cells were studied using the cell-attached and whole-cell configurations of the patch clamp technique. The neurons underlying the glial cells were impaled with either one KCl (2.5 M)-filled microelectrode for voltage recording or two low resistance (1–1.2 MΩ) microelectrodes for stimulation under current clamp and voltage clamp conditions. Pipettes with low resistances were used to minimize the noise generated in the patch clamp recording when the neurons were held under voltage clamp conditions.

The preparation was continuously perfused (1 ml/min) with the following saline (in mM): NaCl, 75; KCl, 5; $MgCl_2$, 8; $CaCl_2$, 8; Tris (pH 7.4), 5 (osmotic pressure ≈200 mOsmol). The bath K^+ content was changed (from 0.1 to 25 mM) without compensating for the osmolarity.

Patch electrodes were filled with a KCl-rich saline containing 80 mM KCl and 5 mM Tris. To perform the cell-attached recordings on K^+-selective channels, 8 mM $CaCl_2$ and 8 mM $MgCl_2$ were added to this saline. The K^+ selectivity of the channels was assessed by replacing part of the KCl by NaCl. In whole-cell experiments, the KCl-rich saline contained 1 mM $MgCl_2$ and 1–100 μM $CaCl_2$ (adjusted with EGTA). Currents and voltages were recorded with a LIST EPC-7 amplifier. Channel currents were filtered (6-pole Bessel filter) at either 2–5 kHz (current-clamped neuron) or 0.2–0.5 kHz (voltage-clamped neuron).

Simultaneous neuron potential measurements performed with a microelectrode and a patch clamp electrode showed that a +16 mV junction potential arose at the tip of the patch electrode in contact with the cytoplasm (Gommerat et al., 1993). The junction potential was not significantly dependent on the patch pipette content (with Na^+ or K^+ as the main cation) but rather on the ionic strength of the pipette-filling saline (Barry & Lynch, 1991). When the K^+ concentration in the pipette was increased to 150 mM, the junction potential decreased to 9 mV. Due to their small size (Gommerat et al., 1993), we were unable to record from glial cells using conventional intracellular microelectrodes. We therefore assumed that the +16 mV shift also occurred in the case of glial cells.

In all the illustrations given here, the traces will be defined as follows: V_N and V_G, intracellular neuronal and glial potential (in either current or voltage clamped cells); I_N and I_G, current through neuronal and glial membrane; I_P, current in cell-attached patch clamp experiments performed on glial cells. Patch potentials are expressed in absolute values: resting cell potential minus applied patch potential. The data given here are the means ± standard errors throughout.

Results

Intracellular Glial Cell Recordings

The electrophysiological criteria used here to identify glial cells in patch clamp experiments have been described previously (Gommerat et al., 1993). Briefly, glial cells were characterized by their large resting potential, high input impedance and lack of excitability. These recordings were obtained on glial cells wrapped around neurons impaled with an intracellular electrode, which are definite criteria in cell identification. In most cases, the sealing of the patch pipette to the glial membranes occurred immediately and spontaneously upon releasing the pressure applied to the pipette before it was dipped in the bath saline. Whole-cell recordings were then obtained by rupturing the patch membrane. This was done by applying either suction or a large, brief (>180 mV) hyperpolarizing pulse to the patch electrode. Examples of intracellular recordings performed in this way are shown in Fig. 1*A*. This glial cell had a resting potential of −72 mV, and responded to current pulses by producing square-shaped voltage changes.

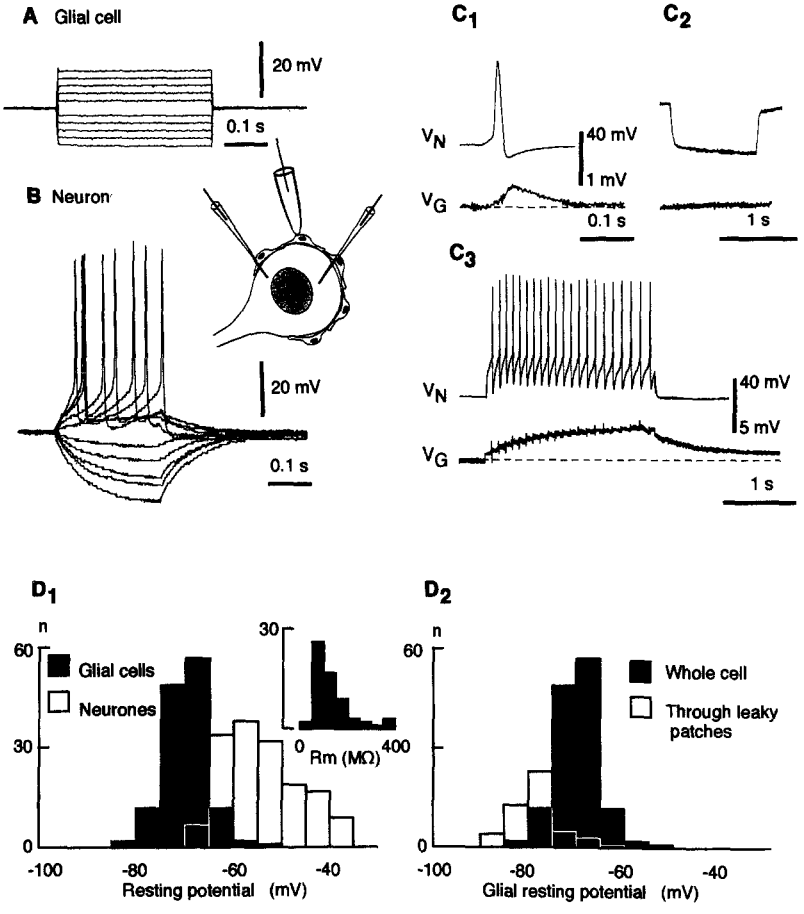

Fig. 1. Intracellular recordings from glial cells and subjacent neurons. (*A* and *B*) The experimental arrangement used is shown in the inset: the glial cell potential was recorded with a patch electrode in the whole-cell configuration while the neuron covered by the glial layer was impaled with two intracellular electrodes. Both series of recordings show voltage changes occurring in response to current pulses applied at increasing 20 pA steps to the glial cell and 2 nA steps to the neuron. Cell resting potential: glial cell: −72 mV; neuron: −58 mV. Input resistance: glial cell: 84 MΩ; neuron: 3.2 MΩ. (*C*) Simultaneous whole-cell recordings on P neurons and their satellite glial cells. In this and subsequent figures, V_N and V_G refer to the membrane potential of neurons and glial cells, respectively. In C_2 and C_3, positive and negative 10 nA current pulses were injected into the neuron, respectively. The spike discharge induced a slowly developing glial cell depolarization, whereas the neuron hyperpolarization did not affect the glial cell voltage. (D_1) Distribution of the cell resting potential in glial cells (black columns, n = 135) and neurons (white columns, n = 156). Bin: 5 mV. Inset: distribution of glial cell input resistance (n = 63). (D_2) Distribution of glial cell resting potential measured either in whole-cell recordings (black columns, same data as in D_1) or through leaky patches (white columns, n = 49, *see text*).

The resulting current-voltage relationship was almost linear and corresponded to an input resistance of 84 MΩ. The recordings in Fig. 1*B* were obtained on the neuron that was covered with the glial cell shown in Fig. 1*A*. They show the great difference between the passive and active properties of the two cell types: in addition to being excitable, the neurons had a small input resistance (3–5 MΩ) and a large time constant (25–70 msec).

The activity of the neurons appeared to have little effect on either the resting potential or the input impedance of the associated glial cells. Isolated spikes produced a delayed 0.5–1.5 mV depolarization of the glial cells (Fig. $1C_1$). This effect summed up in response to neuronal spike bursts, producing a sustained glial depolarization of 2–6 mV (Fig. $1C_3$). After the spike burst, the glial cells recovered their resting potential within 2–5 sec. Neuronal hyperpolarization and subthreshold depolarization induced by injecting current pulses did not affect the glial cells (Fig. $1C_2$), which ruled out the presence of any direct electrical coupling between them.

The histograms in Fig. $1D_1$ show the distribution of the resting potential of glial cells (black columns) and neurons (white columns). The mean resting potential was −69.5 ± 0.4 (n = 135) and −53.4 ± 0.6 (n = 156) in the case of glial cells and neurons, respectively. The glial cell potential was corrected for junction potential (+16 mV) as described in Materials and Methods. The glial cell input resistance ranged from 40 to 380 MΩ; mean: 128 ± 10 MΩ (n = 63) (inset in Fig. $1D_1$).

Although the cell-attached recordings from glial cells remained stable for tens of minutes, the duration of the whole-cell recordings was generally short. This consistently limited the possibility of performing an exhaustive study on the glial cell-neuron interactions. We therefore made use of glial cells having densely packed K^+ channels (*see below*). Some of the patches appeared to contain several tens of channels which were active at the cell resting potential. By switching the patch clamp amplifier to the current clamp mode, we recorded the cell resting potential in a similar way to what occurs with the perforated patch method (Horn & Marty, 1988). Corresponding data are displayed in Fig. $1D_2$ (white columns). The mean resting potential obtained with this method was −77.7 ± 0.7 mV (n = 49), i.e., it was found to be 8 mV larger than in the whole-cell recordings. We did not attempt to find the reason for this difference, but applied a +8 mV shift to the "intracellular recordings" performed through active channels.

The large resting potential of the glial cells suggested that these cells were mainly, if not solely, permeable to K^+ ions. The K^+ selectivity was assessed by perfusing the glial cell-neuron preparation with salines containing varying amounts of K^+ (from 0.1 to 25 mM). In addition to the methods just described, we also deduced the change in glial cell polarization from the change in the unitary current of K^+-selective channels recorded in the cell-attached configuration. One experiment of this kind is illustrated in Fig. 2*A* which relates to a cell-attached patch containing one large (100 pS unitary conductance) K^+ channel. The dependence of the channel unitary current on the cell potential was first assessed by changing the patch voltage. This made it possible to calculate the change in resting potential induced by altering the bath $[K^+]$ from that in the unitary channel current. In Fig. 2*A*, the shift from 5 to 20 mM $[K^+]$ depolarized both neurons and glial cells. The calculated glial depolarization amounted to 33 mV, while that of the neuron was 22 mV. The expected value in the case of a K^+-selective membrane was 35 mV. This experiment also illustrates the difference in the time courses of the K^+-induced voltage changes: the slow neuronal responses may have resulted from K^+ ions having to diffuse through and around the glial layer to reach the neuron.

The $[K^+]$-voltage relationships observed with these various protocols are given in Fig. 2*B*. The continuous curves are the values predicted by the constant-field equation, where the anion contribution is neglected. The ratio of the membrane Na^+ permeability (p_{Na}) to the membrane K^+ permeability (p_K) is: neurons: $p_{Na}/p_K = 0.16$; glial cells: $p_{Na}/p_K = 0.012$.

The glial cells therefore appeared to be predominantly permeable to K^+ ions, particularly when compared with the neurons they covered. This result validates *a posteriori* the use of the K^+ reversal potential as a means of measuring the glial cell resting potential.

Glial Cell Depolarization Induced by Active Neurons

More information about the neuron-glial cell interactions was obtained when large depolarizations were applied to the neuron. For this purpose, the neuron was held under voltage clamp conditions and subjected to 0.5–2 sec voltage pulses. These experiments were carried out on P cells. Hyperpolarizing voltage pulses with an amplitude of 20–80 mV did not produce any detectable changes in the glial cells. In the P cells, depolarizing pulses to positive levels induced large K^+ currents, which displayed a pronounced inactivation. We observed no significant difference between the inactivating rates of the outward currents depending on whether the P cells were endowed with or devoid of glial cells, which meant that the current decrease was mainly due to intrinsic channel properties.

Large outward currents flowing from the neuron depolarized the glial cells (Fig. 3*A*). The glial depolarization was delayed by 0.2–0.3 sec from the peak of the neuronal outward current (inset in Fig. 3*A*). The neuronal outward current was almost immediately deactivated upon repolarization, whereas the glial cell potential slowly returned to its resting level. The slow component of the glial depolarization was fitted to single exponential functions: the corresponding time constant

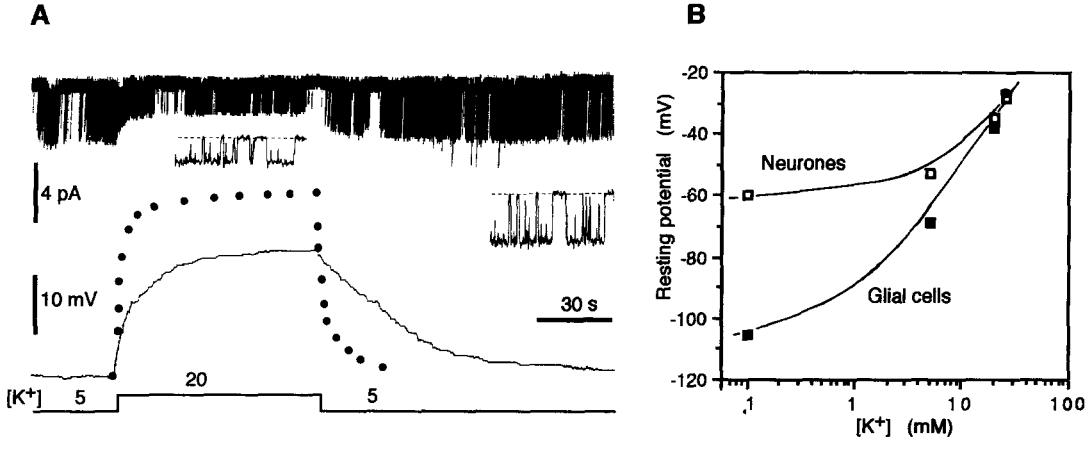

Fig. 2. Effects of external $[K^+]$ on glial and neuronal resting potentials. (*A*) Simultaneous recordings of the unitary current from a cell-attached K^+-selective channel in glial membrane (upper trace) and of the neuron resting potential (continuous trace). The bath K^+ content was transiently increased from 5 to 20 mM, which reduced the channel unitary current (shown on an expanded time base) and depolarized the neuron. The change in the glial cell resting potential (dots superimposed on the neuronal trace) was calculated from the channel unitary current-voltage relationship (*not shown*). (*B*) Cell resting potential-external $[K^+]$ relationships. The continuous curves were drawn according to the constant-field equation, assuming the relative permeability of the p_{Na}/p_K of the neurons to be 0.16 ($n = 23$), and that of the glial cells to be 0.012. ($n = 25$).

was found to be highly variable from one cell to another, ranging from 180 to 1,230 msec.

The following data constitute evidence that the glial depolarization was directly correlated with the size of the neuronal K^+ current. In Fig. 3*B*, the same voltage pulses were applied to a P cell starting with two different holding potentials. The glial cell depolarized in proportion to the size of the outward current induced by the depolarizing pulses and not to the pulse amplitude. The data collected on 12 glial cells endowing P neurons are summarized in Fig. 3*C*, where the glial depolarization is plotted as a function of the neuronal outward current. A close correlation was found to exist (correlation coefficient: 0.9) between both events, measured whether they were at their peak values or upon reaching a steady-state level. When two successive depolarizing pulses were applied to P neurons, the second outward current decreased, due to the inactivation of the K^+ channels by the first pulse. The second glial cell depolarization decreased in the same proportion as that of the neuronal current (Fig. 4*A*). TEA (10 mM) blocked part of the neuronal K^+ current and reduced the glial depolarization in response to the neuronal activation (Fig. 4*B*).

These data are consistent with the widely documented view that K^+ ions accumulate in the interstitial space during neuronal firing, which may lead to cell depolarization. Consequently, the slow glial cell repolarization observed after a neuronal K^+ surge must have paralleled the change in the K^+ equilibrium potential (E_K) undergone by the neuron. This appears to have been the case, as shown in Fig. 4*C*. In this experiment, the voltage-clamped P neuron was held at −60 mV, a positive level with respect to E_K (≈−70 mV), and then subjected to a 100 mV depolarizing pulse. The tail current following the pulse was inward, which might have resulted from the positive shift in the neuronal E_K brought about by the K^+ surge. The tail current decay had almost the same time course as the glial cell repolarization. These data strongly suggest that both events were directly correlated with the clearance of the K^+ ions accumulated in the interstitial space.

Glial Cell Input Resistance

The K^+-induced glial depolarization did not result from a change in the cell input resistance. This is illustrated

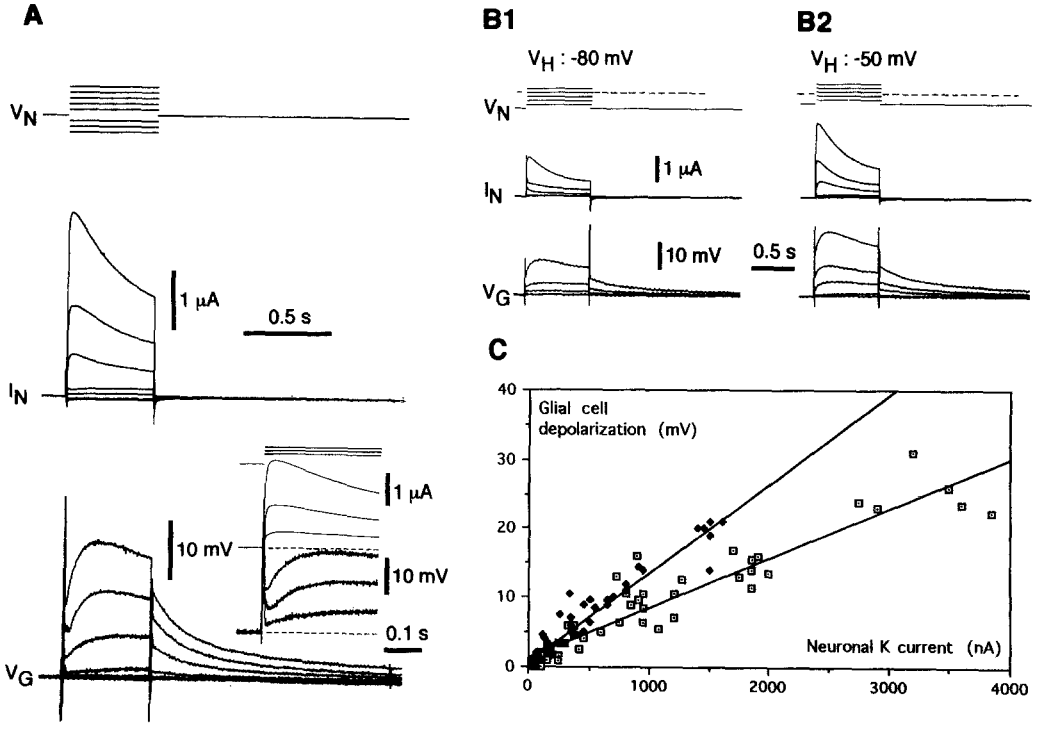

Fig. 3. Patch depolarization induced by neuronal K^+ efflux. (*A*) Neuron held under voltage clamp conditions subjected to depolarizing and hyperpolarizing voltage pulses (trace V_N). Holding potential: −50 mV; pulse amplitude from −60 to +100 mV (20 mV step). I_N: neuronal current elicited in response to the voltage pulses. V_G: glial cell voltage change. Cell resting potential: −70 mV. Inset: details of the neuronal outward current and corresponding glial cell depolarization induced by the three largest depolarizations. (*B*) Same experimental conditions as in *A*. Series of voltage pulses (20 to 100 mV amplitude in 20 mV steps) applied starting from two holding potentials (V_H). Glial cell resting potential: −79 mV. (*C*) Glial cell depolarization as a function of neuronal K^+ current. Open squares: peak values; filled squares: steady-state values. Data pooled from 12 glial cells recorded on 6 P cells. The regression line for steady-state values (correlation coefficient: 0.91) corresponds to a 12.9 mV glial depolarization at 1 µA neuronal K^+ current.

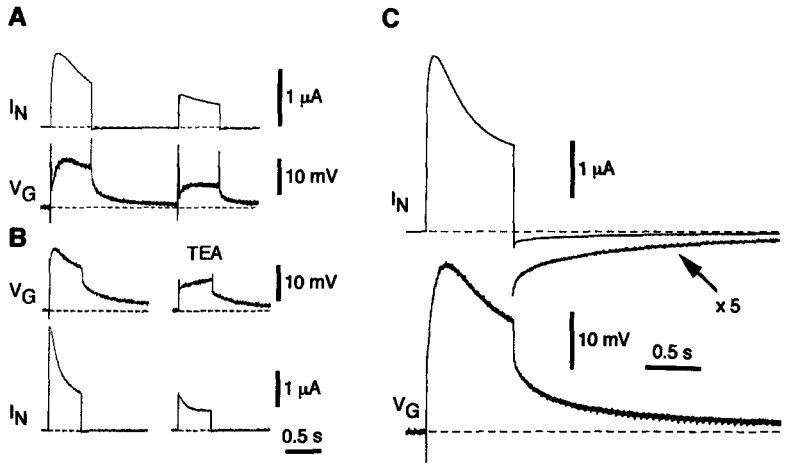

Fig. 4. Relationship between glial cell depolarization and neuronal K^+ current. (*A*) Two successive voltage pulses (100 mV amplitude) were applied to the neuron (holding potential: −50 mV), which inactivated part of the neuronal K^+ current (I_N). V_G: corresponding changes in glial cell voltage. Glial cell resting potential: −78 mV. (*B*) Same experimental conditions as in *A*. Recordings performed before and after adding 10 mM TEA to the bath saline. Glial cell resting potential: −72 mV. (*C*) Glial cell depolarization (V_G) induced by a large neuronal K^+ current (I_N). Neuron voltage clamped at −60 mV. Pulse amplitude: 100 mV. The neuronal tail current (magnified fivefold) has the same time course as the glial cell repolarization. Glial cell resting potential: −66 mV.

in Fig. 5*A*, in which the glial cell input resistance was evaluated by injecting 100 pA inward current pulses. The resulting voltage response remained unchanged during the K^+-induced depolarization.

This finding did not definitely rule out, however, the possible contribution of an active process to the glial response. The input resistance measured under whole-cell conditions did not appear to provide a reliable estimate of the actual membrane properties of the glial cells. This presumably resulted from perineuronal satellites in invertebrates forming a series of cytoplasmic layers around the nerve cells (Fernandez, 1966) and from the existence of electrical coupling between glial cells (Nicaise, 1973). The *in situ* glial cells had an almost linear current-voltage relationship, which was unexpected in the case of a K^+-sensitive membrane working under asymmetrical K^+ conditions. When Cs^+ (1 mM) was present in the bath saline, the *I-V* curve remained almost linear. The predominant K^+ channels that were found to be active in the glial membrane were sensitive to TEA (5–10 mM). Adding TEA (10 mM) to the bath saline had slight effects on the cell input resistance, which increased by less than 10% (Fig. 5*B*).

On a few occasions, moving the patch pipette back to tentatively form outside-out patches detached the glial cell or a large part of it from the neuron and the glial layer. When this occurred while the glial cell was observed under whole-cell current clamp conditions, the cell resting potential remained constant, which showed that the cell separation did not lead to any membrane ruptures. The input resistance of the isolated glial cell amounted to several GΩ (2.5 GΩ in the experiment illustrated in Fig. 5*C*) and the *I-V* curve displayed a pronounced outward rectification that agreed well with the presence of K^+-selective channels.

Glial K^+-selective Channels

With a view to identifying K^+-selective channels, cell-attached patch clamp experiments were performed with pipettes filled with the physiological saline in which K^+ (80 mM) was substituted for Na^+. Under these conditions, the current through K^+ channels reversed its direction at ≈0 mV absolute level, i.e., the patch had to be depolarized by ≈70 mV to compensate for the cell polarization. At the cell resting potential, the K^+ ions

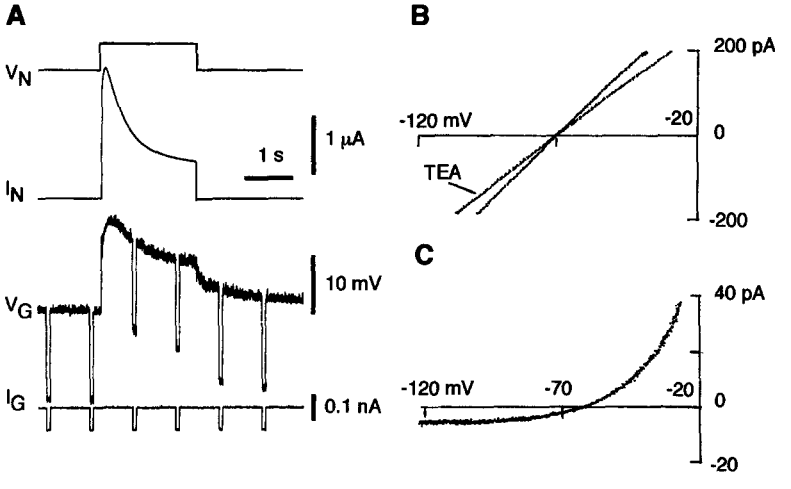

Fig. 5. Passive properties of glial cells. (*A*) Glial cell depolarization (V_G) in response to outward K^+ current (I_N) flowing from the depolarized neuron (V_N: holding potential: −50 mV; 2 sec depolarizing pulse to +50 mV). The glial input resistance was evaluated from the voltage transients induced by 100 pA current pulses (I_G). (*B*) Linear current-voltage relationships from a glial cell bathed in normal saline and after adding 10 mM TEA. Traces obtained by injecting slowly (20 pA/sec) rising current ramp. The cell resting potential (−71 mV) was not affected by TEA. (*C*) Glial cell detached from the preparation. The *I-V* current determined under voltage clamp conditions with a slowly (10 mV/sec) rising voltage ramp displayed a pronounced outward rectification. Cell resting potential: −65 mV.

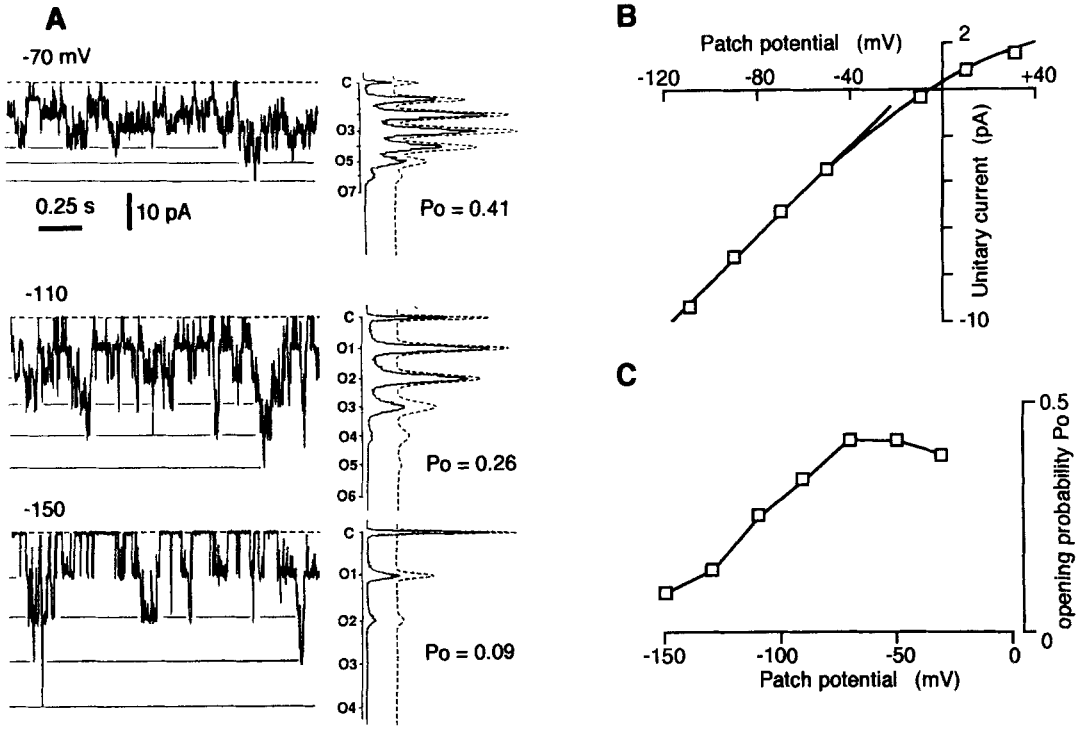

Fig. 6. Cell-attached recording of glial K^+ channels. (*A*) The channel activity was recorded with a patch pipette filled with isotonic KCl. This patch contained seven channels. Voltages are absolute values: glial resting potential (−77 mV, measured at the end of the experiment by rupturing the membrane patch) minus pipette potential. The continuous curves given with the current traces are amplitude histograms; *C:* closed state; 01 to 07: simultaneous opening of one to seven channels. The dotted curves superimposed on the experimental histograms are the expected distribution of seven identical and independent channels having the indicated opening probability P_o. (*B*) Unitary current-voltage relationship. (*C*) Opening probability *vs.* membrane potential in the case of the patch illustrated in *A*.

flowed inwardly. By using a KCl-rich saline in the pipette, K^+ currents could be distinguished from Cl^- currents, whose reversal potential was close to the cell resting level. In about 300 cell-attached patches performed on glial cells, we never observed any active Cl^--selective channels.

The potassium channel most commonly observed (Fig. 6*A*) had a unitary conductance (measured in the negative voltage range) of 103 ± 1.3 pS (n = 40). This channel was present in 94% of the patches (n = 288). The direction of its unitary current was reversed at −5.2 ± 0.5 mV in the presence of 80 mM K^+ in the pipette and at −39 mV with 20 mM K^+. With pipettes filled with isotonic KCl, the channels exhibited a slight inward rectification (Fig. 6*B*); the unitary channel conductance (determined from the slope of the current-voltage curve) decreased to 20 pS at potentials (>80 mV) that induced outward currents.

This channel presumably accounted for the large K^+ permeability of the glial cells. It had a consistent (although extremely variable) opening probability at the cell resting potential and it was present in clusters that might contain several tens of channels. The recordings in Fig. 6*A* are examples of cell-attached recordings from a cluster that contained seven channels. The individual opening probability (P_o) of the channels within a cluster was determined by fitting the experimental amplitude histograms to the distribution predicted by the binomial law, given the observed number of channels. The experimental (continuous curve) and theoretical (dotted curves) distributions are given along with the current traces in Fig. 6*A*. The good fit between the two distributions despite the change in P_o upon large patch hyperpolarization indicates that the clustered channels have identical and independent gating properties. This figure also illustrates the moderate voltage sensitivity of the channel opening probability. Hyperpolarizations of 50–70 mV were required to reduce by half the P_o value observed at the cell resting potential (Fig. 6*C*).

The K^+ channels were recorded from glial cells while the underlying neuron was subjected to depolarizing voltage pulses, as in the previous section. During the neuronal K^+ outflow, the channel unitary current decreased in amplitude as expected from the corresponding glial depolarization. The channel opening probability was not, however, significantly modified during the neuronal depolarization (Fig. 7*A*).

In about 36% of the patches (n = 69), we observed a delayed and persistent increase in the number and opening probability of the K^+ channels after the neuron

depolarization. The activating effect was occasionally large enough to reveal the presence of K^+ channels that remained silent in the absence of neuronal stimulation. The silent channels had the same individual properties as those found to be spontaneously active. This was the case on the experiment shown in Fig. 7*B*, where several large depolarizations were applied to the neuron. Although a few channel openings were present when the neuron was held at its resting level, the large voltage pulses applied to the neuron showed the presence of seven K^+ channels. The channel recruitment started 20–30 sec after the neuron activation, peaked 1–2 min later and vanished within 3–4 min.

All these events occurred after the glial cell had recovered its resting level, as described in the above section. A voltage-dependent process, therefore, did not seem to be primarily involved in the channel opening induced by the neuronal activation, all the less since the glial channels are poorly sensitive to voltage changes. Was the activating process triggered by the K^+-induced glial depolarization? This did not appear to be the case. Glial channel recruitment by active neurons occurred in a limited number of trials, while glial depolarization was systematically observed. Perfusing the neuron-glial preparation with physiological salines containing 20–50 mM K^+, we were able to activate the glial K^+ channels. Since elevated $[K^+]_o$ depolarized both the glial and the neuron, this experiment did not provide any further information about the origin of the channel triggering process. More significantly, when the K^+ pulses were applied while the neuron was held hyperpolarized, thus limiting the K^+-induced neuron depolarization, the glial channel recruitment decreased or was even abolished (Fig. 8*A*). The glial channel activation induced by the

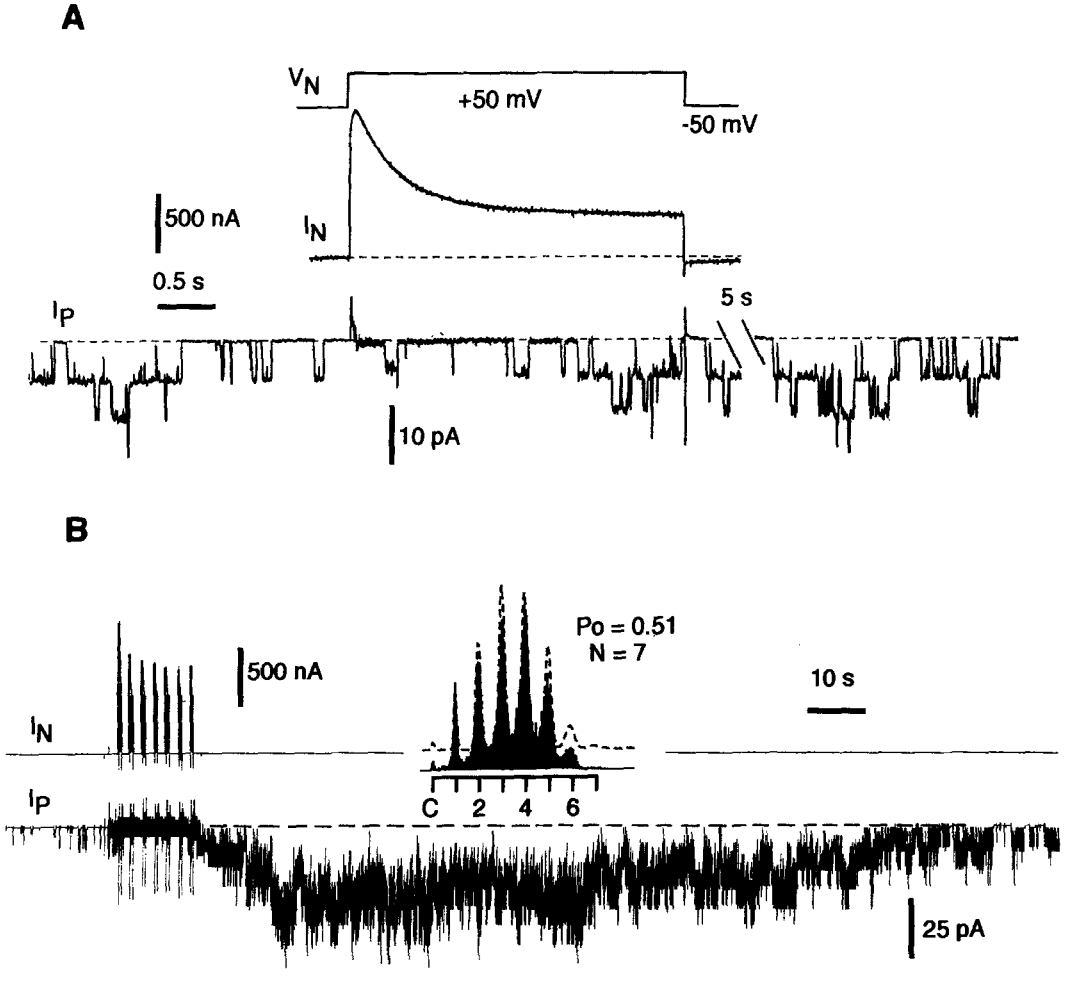

Fig. 7. Changes in glial K^+ channels in response to neuronal depolarization. (*A*) Cell-attached glial channels (I_P) recorded before and during neuron depolarization (V_N) producing a large outward current (I_N). The neuronal K^+ flow reduced the glial unitary current without affecting the channel opening probability. Patch pipette filled with isotonic KCl. No voltage applied to the pipette. (*B*) Voltage pulses (80 mV) producing large outward currents in the neuron (I_N) induced a delayed and persistent increase in the glial channel opening (I_P). The amplitude histogram shows that the neuronal depolarization activated seven channels. Patch pipette: isotonic KCl; patch potential: −110 mV (absolute value).

neuron depolarization (under voltage clamp condition or in response to $[K^+]_o$) was strongly reduced when the bath saline contained 16 mM Mg^{2+} and 0.1 mM Ca^{2+} instead of 8 mM each (Fig. 8*B*). These findings indicate that the neuronal depolarization was a prerequisite for the glial channel activation, that the channel activation was not mediated by the K^+-induced glial depolarization, and that the neuron presumably released a signal in a calcium-dependent way.

Discussion

The results we collected in the present study with our neuron-glial preparation substantiate earlier views on the K^+ dynamics in interstitial spaces and provide some new information about the way in which glial cells may participate in ionic homeostasis.

Neuronal firing-induced glial depolarization has been observed in various systems (Orkand, Orkand & Tang, 1981; Walz & MacVicar, 1988). In our preparation, the depolarization appeared to be directly correlated with the amount (or more precisely with the flux) of K^+ from the neurons covered with glial cells. We observed a consistent quantitative relationship between these two events. The main difference with the previously published data concerns the amplitude of the K^+-induced glial depolarization and its time course. Except when K^+ ions were forced from the neurons by applying large voltage clamp pulses, repeated neuronal firing induced only moderate glial depolarization (2–6 mV) and the glial cells recovered their resting level within about 1 sec. The K^+ clearance in the interstitial space, therefore, appears to have occurred much more quickly than those measured with ion-sensitive microelectrodes *in situ* or in tissue slices (*see, for instance,* Orkand et al., 1966; Coles & Orkand, 1983; Ballanyi, Grafe & Ten Bruggencate, 1987), where it lasted for several tens of seconds or even longer.

The fast K^+ clearance we observed may have been due to K^+ uptake by the surrounding glial cell layer and to its direct diffusion into the extracellular space. The mechanical methods we used to discard the connective sheath may also have partly detached the glial layer from the neuron, thus facilitating its passive diffusion. On the other hand, we also observed that the glial cells are highly permeable to K^+ ions. Both facts may account for the fast return of the interstitial $[K^+]$ to its resting level.

The finding that molluscan glial cells have a high resting potential and behave like almost perfect K^+ electrodes are in line with data published by several investigators (Kuffler et al., 1966; Kettenmann, Sonnhof & Schachner, 1983; Walz, Wuttke & Hertz, 1984). The high K^+ selectivity results from the presence of densely clustered K^+ channels. The main K^+ channel we observed had characteristic inward rectifying properties under symmetrical ionic conditions (isosmotic K^+ in the patch pipette). This channel accounts for more than 95% of the K^+ current through the glial membrane.

Inwardly rectifying K^+ channels have been detected in almost all vertebrate glial cells (*review by* Barres

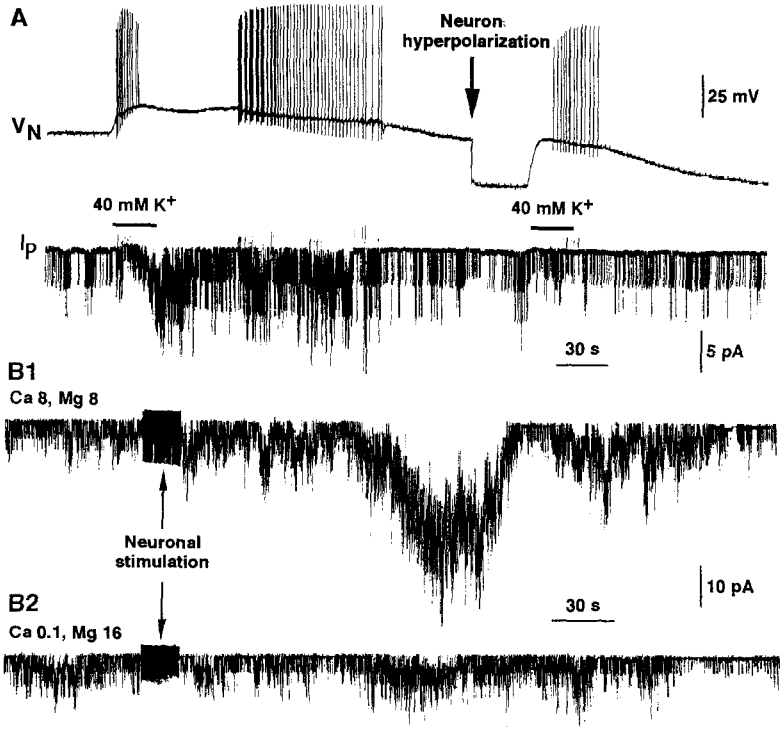

Fig. 8. Recruitment of glial K^+ channels may involve a signal released by active neurons. (*A*) Simultaneous recordings of a P cell membrane potential (V_N) and of K^+ channels (I_P) from its satellite glial cells. Patch pipette: isotonic KCl; patch hyperpolarized by 20 mV. Brief pulses of physiological saline containing 40 mM K^+ were applied to the preparation. The first pulse depolarized and fired the neuron and increased the glial channel activity. The second K^+ pulse was applied while the neuron was hyperpolarized from its resting level (−50 mV) to −80 mV, which prevented the glial channels from being activated by the K^+ pulse. (*B*) Cell-attached recording of glial K^+ channels in response to neuronal firing induced by applying depolarizing voltage pulses (50 mV − 50 msec − 4 Hz for 20 sec). Patch pipette: isotonic KCl; no voltage applied to the patch membrane. Neuronal stimulation increased NP_o, measured in 120 sec samples, from 0.093 ± 0.020 to 0.661 ± 0.044 when the ganglion was in normal saline (*B1*), whereas NP_o was not significantly modified (from 0.081 ± 0.012 to 0.097 ± 0.014) in low Ca^{2+}-high Mg^{2+} saline (*B2*).

et al., 1990). The main difference with the molluscan channel lies in the amount of rectification. Although the inward rectification is an intrinsic property of the channel since it was observed with symmetrical $[K^+]$, the inward rectification turned into outward in the presence of physiological $[K^+]_o$. This gives isolated glial cells their outward going whole-cell current voltage relationship. Consequently, in the molluscan K^+ channel, K^+ ions flow outwardly under physiological conditions and inwardly in the presence of local $[K^+]_o$ increase. The same channels are therefore potentially able to play both functions as far as they are actually involved in K^+ siphoning, according to the "spatial buffering" hypothesis.

The gating properties of the K^+ channels are still obscure. We observed that the channels were either spontaneously active or that they opened in response to the neuronal stimulation. When active, the opening probability of the channels was found to be highly variable and only slightly dependent on the membrane potential. These active channels presumably gave the glial cells their K^+ selectivity. Applying stimulation to the underlying neuron increased the opening probability of active channels and unmasked silent channels. This effect occurred with a latency of 20–30 sec and persisted for several minutes. In the framework of the K^+ homeostasis hypothesis, the delayed increase in K^+ channel activity might help to eliminate the K^+ ions accumulated in the glial layer during the neuronal firing.

Several facts indicate that the triggering mechanism may involve the existence of a neuron-to-glial signal. The channel activation induced by brief neuronal depolarizations occurred after the glial cell had recovered from the K^+-induced depolarization. In addition, since the channels were found to be poorly sensitive to voltage changes, a purely voltage-dependent gating mechanism appears to be unlikely. Could the accumulated K^+ be the signal? The channels were observed on the glial membrane not facing the neuron. They were included in the patch pipette and were therefore inaccessible to $[K^+]_o$ changes. Consequently, the possibility that the channels may have been directly activated by K^+ ions can be ruled out. These findings also indicate that the triggering process must act on the cytoplasmic side of the channels. The K^+-induced glial depolarization may have open voltage-dependent Ca channels, whose presence has been described in various glial cell types (MacVicar, 1984; Amédée et al., 1991; Berger et al., 1992). The subsequent increase in glial $[Ca]_i$ may open Ca-dependent K^+ channels (Quandt & MacVicar, 1986). Additional data are required to evaluate whether the molluscan K^+ channels are regulated by $[Ca]_i$. That K^+ channel opening in response to pulses of K^+-rich saline was abolished when the underlying neuron was held in the hyperpolarized state points to the existence of a signal emanating from the neuron. This signal was apparently absent in the presence of low Ca^{2+}-high Mg^{2+}, which would indicate that its release was induced by the entry of calcium in the neuron. Based on data obtained by recording glial cell activities at the surface of the frog optic nerve, Marrero et al. (1989) hypothesized that unidentified chemical factors released by the active axon may have altered the glial sodium channels. If a signal of this kind (*see also* Barres et al., 1990) is released by the active molluscan neurons, it might act on glial receptors that might in turn open the K^+ channels by triggering an intracellular glial signal.

This work was supported by the CNRS and by a grant from the Fondation pour la Recherche Médicale. We would like to thank Mrs. M. André and Mr. G. Jacquet for technical assistance and Mrs. J. Blanc for improving the English.

I. Gommerat is recipient of a fellowship from the Ministère de la Recherche et de la Technologie.

References

Amédée, T., Ellie, E., Dupouy, B., Vincent, J.D. 1991. Voltage-dependent calcium and potassium channels in Schwann cells cultured from dorsal root ganglia of the mouse. *J. Physiol.* **441:**35–56

Ballanyi, K., Grafe, P., Ten Bruggencate, G. 1987 Ion activities and potassium uptake mechanisms of glial cells in guinea-pig olfactory cortex slices. *J. Physiol.* **382:**159–174

Barres, B.A. 1991. New roles for glia. *J. Neurosci.* **11:**3685–3694

Barres, B.A., Chun, L.L.Y., Corey, D.P. 1988. Ion channel expression by white matter glia: I. Type 2 astrocytes and oligodendrocytes. *Glia* **1:**10–30

Barres, B.A., Chun, L.L.Y., Corey, D.P. 1990. Ion channels in vertebrate glia. *Annu. Rev. Neurosci.* **13:**441–474

Barry, P.H., Lynch, J.W. 1991. Liquid junction potentials and small cell effects in patch-clamp analysis. *J. Membrane Biol.* **121:** 101–117

Berger, T., Schnitzer, J., Kettenmann, H. 1991. Developmental changes in the membrane current pattern, K^+ buffer capacity, and morphology of glial cells in the *corpus callosum* slice. *J. Neurosci.* **11:**3008–3024

Berger, T., Schnitzer, J., Orkand, P.M., Kettenmann, H. 1992. Sodium and calcium currents in glial cells of the mouse *corpus callosum* slice. *Eur. J. Neurosci.* **4:**1271–1284

Bevan, S., Chiu, S.Y., Gray, P.T.A., Ritchie, J.M. 1985. The presence of voltage-gated sodium, potassium and chloride channels in rat cultured astrocytes. *Proc. R. Soc. Lond. B* **225:**299–313

Bevan, S., Raff, M. 1985. Voltage-dependent potassium currents in cultured astrocytes. *Nature* **315:**229–232

Brew, H., Gray, P.T.A., Mobbs, P., Attwell, D. 1986. Endfeet of retinal glial cells have higher densities of ion channels that mediate K buffering. *Nature* **324:**466–468

Chiu, S.Y. 1991. Functions and distribution of voltage-gated sodium and potassium channels in mammalian Schwann cells. *Glia* **4:**541–558

Chiu, S.Y., Schrager, P., Ritchie, J.M. 1984. Neuronal-type Na^+ and K^+ channels in rabbit cultured Schwann cells. *Nature* **311:** 156–157

Coles, J.A., Orkand, R.K. 1983. Modification of potassium movement through the retina of the drone (*Apis Mellifera*) by glial uptake. *J. Physiol.* **340:**157–174

Fernandez, J. 1966. Nervous system of the snail *Helix aspersa*. I.

Structure and histochemistry of ganglionic sheath and neuroglia. *J. Comp. Neur.* **127:**157–182

Gola, M., Niel, J.P., Delmas, P., Jacquet, G. 1993. Satellite glial cells *in situ* within mammalian prevertebral ganglia express K^+ channels active at rest potential. *J. Membrane Biol.* **136:**75–84

Gommerat, I., Jacquet, G., Chagneux, H., Gola, M. 1993. Single-channel and whole-cell recordings from on-neurone glial cells in *Helix pomatia* ganglia. *J. Neurosci. Meth.* **50:**243–251

Horn, R., Marty, A. 1992. Muscarinic activation of ionic currents measured by a new whole-cell recording method. *J. Gen. Physiol.* **92:**145–159

Jalonen, T., Holopainen, I. 1989. Properties of single potassium channels in cultured primary astrocytes. *Brain Res.* **484:**177–183

Kettenmann, H., Orkand, R.K., Lux, H.D. 1984. Some properties of single potassium channels in cultured oligodendrocytes. *Pfluegers Arch.* **400:**215–221

Kettenmann, H., Orkand, R.K., Lux, H.D., Schachner, M. 1982. Single potassium channel currents in cultured mouse oligodendrocytes. *Neurosci. Lett.* **32:**41–46

Kettenmann, H., Sonnhof, U., Schachner, M. 1983. Exclusive potassium dependence of the membrane potential in cultured mouse oligodendrocytes. *J. Neurosci.* **3:**500–505

Konishi, T. 1989. Voltage-dependent potassium channels in mouse Schwann cells. *J. Physiol.* **411:**115–130

Kuffler, S.W., Nicholls, J.G., Orkand, R.K. 1966. Physiologic properties of glial cells in the central nervous system of amphibia. *J. Neurophys.* **29:**768–787

Marrero, H., Astion, M.L., Coles, J.A., Orkand, R.K. 1989. Facilitation of voltage-gated ion channels in frog neuroglia by nerve impulses. *Nature* **339:**378–380

Marrero, H., Orkand, P.M., Kettenmann, H., Orkand, R.K. 1991. Single channel recording from glial cells on the untreated surface of the frog optic nerve. *Eur. J. Neurosci.* **3:**813–819

McLarnon, J.G., Kim, S.U. 1989. Single channel potassium currents in cultured adult bovine oligodendrocytes. *Glia* **2:**298–307

MacVicar, B.A. 1984. Voltage-dependent calcium channels in glial cells. *Science* **226:**1345–1347

Murphy, S., Pearce, B. 1987. Functional receptors for neurotransmitters on astroglial cells. *Neuroscience* **22:**381–394

Newman, E.A. 1986. Regional specialization of the membrane of retinal glial cells and its importance to K^+ spatial buffering. *Ann. NY Acad. Sci.* **481:**273–286

Nicaise, G. 1973. The gliointerstitial system of molluscs. *Int. Rev. Cytol.* **34:**251–332

Nilius, B., Reichenbach, A. 1988. Efficient K^+ buffering by mammalian retinal glial cells is due to cooperation of specialized ion channels. *Pfluegers Arch.* **411:**654–660

Nowak, L., Ascher, P., Berwald-Netter, Y. 1987. Ionic channels in mouse astrocytes in culture. *J. Neurosci.* **7:**101–109

Orkand, R.K., Nicholls, J.G., Kuffler, S.W. 1966. Effect of nerve impulses on the membrane potential of glial cells in the central nervous system of amphibia. *J. Neurophys.* **29:**788–806

Orkand, R.K., Orkand, P.M., Tang, C.-M. 1981. Membrane properties of neuroglia in the optic nerve of *Necturus*. *J. Exp. Biol.* **95:**49–59

Pin, T., Crest, M., Ehile, E., Jacquet, G., Gola, M. 1990. Plateau-generating nerve cells in *Helix:* morphological and electrophysiological characteristics. *J. Exp. Biol.* **152:**189–209

Quandt, F.N., MacVicar, B.A. 1986. Calcium activated potassium channels in cultured astrocytes. *Neuroscience* **19:**29–41

Ritchie, J.M. 1992. Voltage-gated ion channels in Schwann cells and glia. *TINS* **15:**345–351

Soliven, B. Szuchet, S., Arnason, B.G., Nelson, D.J. 1988. Voltage-gated potassium currents in cultured ovine oligodendrocytes. *J. Neurosci.* **8:**2131–2141

Sonnhof, U., Schachner, M. 1986. Single voltage-dependent K^+-channels in cultured astrocytes. *Neurosci. Lett.* **64:**241–246

Sontheimer, H., Kettenmann, H. 1988. Heterogeneity of potassium currents in cultured oligodendrocytes. *Glia* **1:**415–420

Steinhäuser, C., Berger, T., Frotscher, M., Kettenmann, H. 1992. Heterogeneity in the membrane current pattern of identified glial cells in the hippocampal slice. *Eur. J. Neurosci.* **4:**472–484

Walz, W. 1989. Role of glial cells in the regulation of the brain ion microenvironment. *Prog. Neurobiol.* **33:**309–333

Walz, W., MacVicar, B.A. 1988. Electrophysiological properties of glial cells: Comparison of brain slices with primary cultures. *Brain Res.* **443:**321–324

Walz, W., Wuttke, W., Hertz, L. 1984. Astrocytes in primary cultures: membrane potential characteristics reveal exclusive potassium conductance and potassium accumulator properties. *Brain Res.* **292:**367–374

Wilson, G.F., Chiu, S.Y. 1990. Regulation of potassium channels in Schwann cells during early developmental myelinogenesis. *J. Neurosci.* **10:**1615–1625